

# Prediction of quantum stripe ordering in optical lattices

Congjun Wu,<sup>1</sup> W. Vincent Liu,<sup>2</sup> Joel Moore,<sup>3,4</sup> and Sankar Das Sarma<sup>5</sup>

<sup>1</sup>*Kavli Institute for Theoretical Physics, University of California, Santa Barbara, CA 93106*

<sup>2</sup>*Department of Physics and Astronomy, University of Pittsburgh, Pittsburgh, PA 15260*

<sup>3</sup>*Department of Physics, University of California, Berkeley, CA 94720*

<sup>4</sup>*Materials Sciences Division, Lawrence Berkeley National Laboratory, Berkeley CA 94720*

<sup>5</sup>*Condensed Matter Theory Center, Department of Physics, University of Maryland, College Park, MD 20742*

We predict the robust existence of a novel quantum orbital stripe order in the  $p$ -band Bose-Hubbard model of two-dimensional triangular optical lattices with cold bosonic atoms. An orbital angular momentum moment is formed on each site exhibiting a stripe order both in the superfluid and Mott-insulating phases. The stripe order spontaneously breaks time-reversal, lattice translation and rotation symmetries. In addition, it induces staggered plaquette bond currents in the superfluid phase. Possible signatures of this stripe order in the time of flight experiment are discussed.

PACS numbers: 03.75.Lm, 05.30.Jp, 73.43.Nq, 74.50.+r

Cold atomic systems with multiple components, such as large spin systems, exhibit much richer phase diagrams and properties than the usual spinless bosons and spin- $\frac{1}{2}$  fermions. For example, various spinor condensations and spin dynamics have been investigated [1, 2]. Similarly, large spin fermions also exhibit novel features, including hidden symmetries [3], quintet Cooper pairing states [4], and multiple-particle clustering instabilities [5]. Motivated by such considerations, but for orbital degeneracy, we investigate the  $p$ -band Bose-Hubbard (BH) model for cold atom optical lattices, finding a novel quantum orbital stripe phase in triangular  $p$ -band optical lattices.

In solid state physics, orbital dynamics plays important roles in transition metal oxides leading to interesting phenomena, such as orbital ordering and colossal magnetoresistance [6]. In optical lattices, pioneering experiments on orbital physics have been recently carried out by Browaeys *et. al* [7] by accelerating the lattice of bosons, and by Kohl *et. al* [8] by using fermionic Feshbach resonance. These experiments demonstrate the population of higher orbital bands, motivating our theoretical interest in possible orbital ordering in optical lattices. Compared to transition metal oxides where Jahn-Teller distortions often remove the orbital degeneracy, optical lattices have the advantage of the lattice rigidity, and thus the orbital degeneracy is robust. The  $p$ -band bosons in the square or cubic lattices, have received much attention [9, 10, 11, 12]. For example, Ref. [10] focuses on the sub-extensive  $Z_2$  symmetry [13, 14, 15] and the resulting nematic superfluid order by considering only the  $\sigma$ -type bonding in the band structure. By further keeping the  $\pi$ -bonding term, the ground state is shown to break time reversal (TR) symmetry spontaneously, forming an antiferromagnetic order of orbital angular momentum (OAM) moments [11, 12].

The  $p$ -band bosons in a frustrated optical lattice have, however, never been studied before. The experimental realization of the 2D triangular lattice has been discussed

in the literature [16]. In this paper, we find a novel quantum stripe ordering of the  $p$ -band bosons in such a lattice. The onsite Hubbard interaction gives rise to a Hund's rule-like coupling in the OAM channel, resulting in the formation of an Ising OAM moment on each site. Due to the geometric frustration, the ground state exhibits a stripe order of the OAM moments which spontaneously breaks TR, lattice rotation and translation symmetries. This stripe order bears some superficial similarity to its solid-state counterpart observed in strongly correlated electronic systems, such as manganites [17], high  $T_c$  cuprates [18], and high-Landau level quantum Hall systems [19], but is different qualitatively since, unlike the solid-state examples, the stripe order in the  $p$ -band bosonic triangular optical lattices is fully quantum in nature and does not just arise from the long-range Coulomb interaction.

We begin with the construction of the  $p$ -band BH model in a 2D ( $x$ - $y$ ) triangular lattice. The optical potential on each site is approximated by a 3D anisotropic harmonic potential with frequencies  $\omega_z \gg \omega_x = \omega_y = \omega_{xy}$ . Thus we can neglect the  $p_z$ -band, and only consider a two-band model of  $p_x$  and  $p_y$ . We define three unit vectors  $\hat{e}_1 = \hat{e}_x$ ,  $\hat{e}_{2,3} = -\frac{1}{2}\hat{e}_x \pm \frac{\sqrt{3}}{2}\hat{e}_y$ , and the two primitive lattice vectors can be taken as  $a\hat{e}_{1,2}$  ( $a$  the lattice constant). The projection of the  $p_{x,y}$  orbitals along the  $\hat{e}_{1,2,3}$  directions are  $p_1 = p_x$ ,  $p_{2,3} = -\frac{1}{2}p_x \pm \frac{\sqrt{3}}{2}p_y$ . Due to the anisotropic nature of the  $p$ -orbitals, the hopping terms are dominated by the "head to tail" type  $\sigma$ -bonding (the  $\pi$ -bonding  $t_\perp$  term can be neglected here) as

$$H_0 = t_\parallel \sum_{\vec{r}, i=1,2,3} \left\{ p_{i,\vec{r}}^\dagger p_{i,\vec{r}+\hat{e}_i} + h.c. \right\}, \quad (1)$$

where  $t_\parallel$  is positive due to the odd parity of the  $p$ -orbitals. The on-site Hubbard repulsion  $H_{int}$  can be calculated

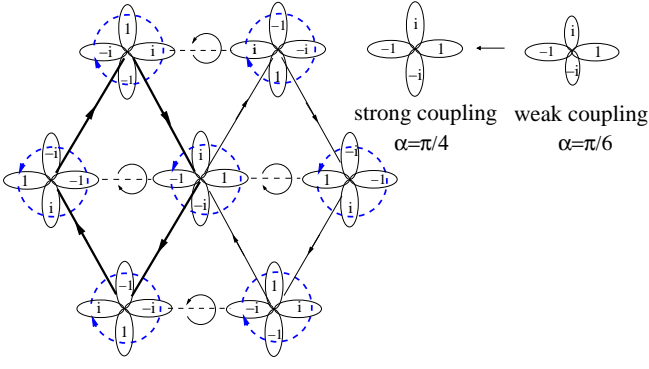


FIG. 1: The condensate configuration in the real space described by Eq.(3) with TR, rotation, and  $U(1)$  symmetry breaking. The unit cell contains 4 sites as marked with thick lines. The OAM moments (dashed arrowed circles) form the stripe order, and induce bond currents exhibiting staggered plaquette moments (solid arrowed circles).  $\alpha$  in Eq. 3 depends on the interaction strength with  $\alpha = \frac{\pi}{6}(\frac{\pi}{4})$  in the weak (strong) coupling limit respectively. Currents vanish in the weak coupling limit, and exist on tilted bonds at finite interaction strength with directions specified by arrows.

from the contact interaction of coupling constant  $g$ :

$$H_{int} = \frac{U}{2} \sum_{\vec{r}} \left\{ n_{\vec{r}}^2 - \frac{1}{3} L_{z,\vec{r}}^2 \right\}, \quad (2)$$

with  $n_{\vec{r}}$  the particle number and  $L_z = -i(p_x^\dagger p_y - p_y^\dagger p_x)$  the  $z$ -component OAM;  $U = 3g/[4(2\pi)^{3/2} l_x l_y l_z]$  with  $l_i = \sqrt{\hbar/(m\omega_i)}$  ( $i = x, y, z$ ). The important feature of  $H_{int}$  is its ferro-orbital nature [11] which is analogous to the Hund's rule for atomic electrons. This implies that bosons on each site prefer to go into the axial states of  $p_x \pm ip_y$ . This is because the axial states are spatially more extended than the polar states  $p_{x,y}$ , and thus are energetically more favorable for  $g > 0$ .

We first consider the weak coupling limit,  $U/t \rightarrow 0$ . The Brillouin zone takes the shape of a regular hexagon with the edge length  $4\pi/(3a)$ . The energy spectrum of  $H_0$  is  $E(k) = t_{\parallel} \left\{ f_{\vec{k}} \mp \sqrt{f_{\vec{k}}^2 - 3g_{\vec{k}}^2} \right\}$ , where  $f_{\vec{k}} = \sum_{i=1}^3 \cos(\vec{k} \cdot \hat{e}_i)$  and  $g_{\vec{k}} = \sum_{3 \geq i > j \geq 1} \cos(\vec{k} \cdot \hat{e}_i) \cos(\vec{k} \cdot \hat{e}_j)$ . The spectrum contains three degenerate minima located at  $K_1 = (0, \frac{2\pi}{\sqrt{3}a})$ ,  $K_{2,3} = (\pm \frac{\pi}{a}, \frac{\pi}{\sqrt{3}a})$ . The factor  $e^{i\vec{K}_1 \cdot \vec{r}}$  takes the value of  $\pm 1$  uniformly in each horizontal row but alternating in adjacent rows. If the above pattern is rotated at angles of  $\pm \frac{2\pi}{3}$ , then we arrive at the patterns of  $e^{i\vec{K}_{2,3} \cdot \vec{r}}$ . Each eigenvector is a 2-component superposition vector of  $p_x$  and  $p_y$  orbitals. The eigenvectors at energy minima are  $\psi_{K_1} = e^{i\vec{K}_1 \cdot \vec{r}} |p_y\rangle$ .  $\psi_{K_{2,3}}$  can be obtained by rotating  $\psi_1$  at angles of  $\pm \frac{2\pi}{3}$  respectively.

The ground state condensate wavefunction  $\Psi_c$  can be constructed as follows. Any linear superposition of the three band minima  $\Psi_c(\vec{r}) = c_1 \psi_{K_1} + c_2 \psi_{K_2} + c_3 \psi_{K_3}$  with the constraint  $|c_1|^2 + |c_2|^2 + |c_3|^2 = 1$  equally min-

imizes the kinetic energy  $H_0$ . However, an infinitesimal  $U/t$  removes the band degeneracy to further optimize the interaction energy  $H_{int}$ . After straightforward algebra, we find the optimal configurations occur at  $c_1 = 0$ ,  $c_2 = \frac{1}{\sqrt{2}}$ ,  $c_3 = \frac{i}{\sqrt{2}}$ , and its symmetrically equivalent partners. Thus the mean field condensate can be expressed as  $\frac{1}{\sqrt{N_0!}} \left\{ \frac{1}{\sqrt{2}} (\psi_{K_2}^\dagger + i\psi_{K_3}^\dagger) \right\}^{N_0} |0\rangle$  with  $|0\rangle$  the vacuum state and  $N_0$  the particle number in the condensate. This state breaks the  $U(1)$  gauge symmetry, as well as TR and lattice rotation symmetries, thus the ground state manifold is  $U(1) \otimes Z_2 \otimes Z_3$ . This state also breaks lattice translation symmetry, which is, however, equivalent to suitable combinations of  $U(1)$  and lattice rotation operations.

For better insight, we transform the above momentum space condensate to the real space. The orbital configuration on each site reads

$$e^{i\phi_{\vec{r}}} (\cos \alpha |p_x\rangle + i\sigma_{\vec{r}} \sin \alpha |p_y\rangle) \quad (3)$$

with  $\alpha = \frac{\pi}{6}$  as  $U/t \rightarrow 0$ . The general configuration of  $\alpha$  is depicted in Fig. 1 for later convenience. The  $U(1)$  phase  $\phi_{\vec{r}}$  is specified at the right lobe of the  $p$ -orbital. The Ising variable  $\sigma_{\vec{r}} = \pm 1$  denotes the direction of the OAM, and is represented by the anti-clockwise (clockwise) arrow on each site. Each site exhibits a nonzero OAF moment and breaks TR symmetry. At  $U/t \rightarrow 0$ ,  $p_{x,y}$  are not equally populated, and the moment per particle is  $\frac{\sqrt{3}}{2}\hbar$ . This does not fully optimize  $H_{int}$  which requires  $L_{z,\vec{r}} = \pm\hbar$ . However, it fully optimizes  $H_0$  which dominates over  $H_{int}$  in the weak coupling limit. We check that the phase difference is zero along each bond, and thus no inter-site bond current exists. Interestingly, as depicted in Fig. 1, OAM moments form a stripe order along each horizontal row. The driving force for this stripe formation in the SF regime is the kinetic energy, i.e., the phase coherence between bosons in each site. By contrast, the stripe formation in high  $T_c$  cuprates is driven by the competition between long range repulsion and the short range attraction in the interaction terms [18].

Next we discuss the ordering at large large values of  $U/t$ . We first minimize  $H_{int}$  with  $n$  particles per site. For simplicity, we consider the large  $n$  case, then Hund's rule coupling favors the onsite state  $\frac{1}{\sqrt{n!}} \left\{ (\cos \frac{\pi}{4} p_x^\dagger + i\sigma_r \sin \frac{\pi}{4} p_y^\dagger) \right\}^n |0\rangle$ . This corresponds to the case  $\alpha = \frac{\pi}{4}$  in Fig. 1. Because of the anisotropic orientation of the  $p$ -orbitals, the phase difference between two sites along each bond not only depends on the  $U(1)$  and the Ising variables, but also on the direction of the bond as in the  $p + ip$  Josephson junction arrays [13]. This effect can be captured by a  $U(1)$  gauge field. The effective Hamiltonian then reads  $H_{\text{eff}} = -\frac{1}{2} n t_{\parallel} \sum_{\langle \vec{r}_1, \vec{r}_2 \rangle} \cos \{ \phi_{\vec{r}_1} - \phi_{\vec{r}_2} - A_{\vec{r}_1, \vec{r}_2} (\sigma_{\vec{r}_1}, \sigma_{\vec{r}_2}) \} + \frac{1}{3} U \sum_{\vec{r}} n_{\vec{r}}^2$ , where the gauge field  $A_{\vec{r}_1, \vec{r}_2} = \sigma_{\vec{r}_1} \theta_{\vec{r}_1, \vec{r}_2} - \sigma_{\vec{r}_2} \theta_{\vec{r}_2, \vec{r}_1}$ ;  $\theta_{\vec{r}_1, \vec{r}_2}$  is the angle between the bond from  $\vec{r}_1$  to  $\vec{r}_2$  and the  $x$ -axis, and thus

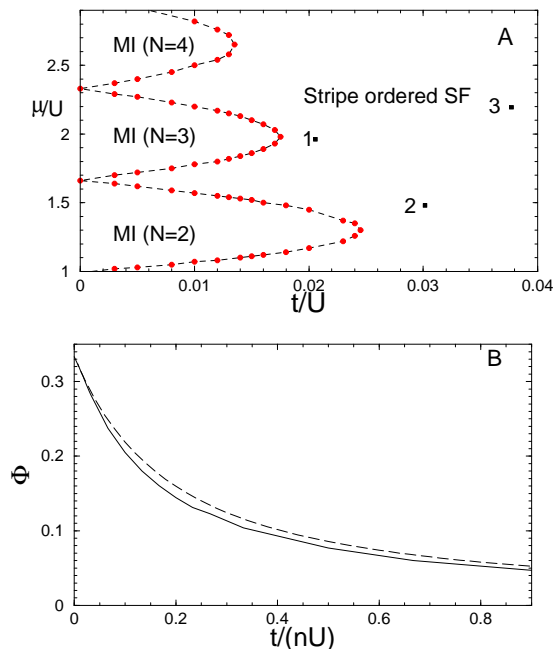


FIG. 2: A) Phase diagram based on the GMF theory in the  $2 \times 2$  unit cell (see Fig. 1). Large scale GMF calculations in a  $30 \times 30$  lattice are performed to confirm the stripe ordered superfluid (SF) phase at points 1, 2 and 3 with  $(t/U, \mu/U) = (0.02, 2), (0.03, 1.5)$  and  $(0.038, 2.2)$ , respectively. B) The flux  $\Phi$  around a rhombic plaquette v.s.  $t/(nU)$ . It decays from  $\frac{1}{3}$  in the strong coupling limit to 0 in the non-interaction limit. The solid line is the GMF result at  $n = 3$ , while the dashed line is based on the energy function Eq. 5 of the trial condensate.

$\theta_{\vec{r}_2, \vec{r}_1} = \theta_{\vec{r}_1, \vec{r}_2} + \pi$ . The external gauge flux in the plaquette  $i$  with three vertices  $\vec{r}_{1,2,3}$  can be calculated as

$$\Phi_i = \frac{1}{2\pi} \sum_{\langle r, r' \rangle} A_{r, r'} = \frac{1}{6} (\sigma_{\vec{r}_1} + \sigma_{\vec{r}_2} + \sigma_{\vec{r}_3}) \text{ mod } 1. \quad (4)$$

Following the analysis in Ref. [13, 20], the ground state configuration for Ising variables requires the flux  $\Phi_i$  (vorticity) in each plaquette to be as small as possible, which are just  $\pm \frac{1}{6}$  corresponding to Ising variables of two  $\pm 1$ 's and one  $\mp 1$ .

The stripe order persists in the strong coupling SF regime due to the interaction among vortices. Consider a plaquette with vorticity  $+\frac{1}{6}$ , thus its three vertices are with two  $+1$ 's and one  $-1$ . The neighbouring plaquette sharing the edge with two  $+1$ 's must have the same vorticity, and merges with the former one to form a rhombic plaquette with the total vorticity  $+\frac{1}{3}$ . Thus the ground state should exhibit a staggered pattern of rhombic plaquettes with vorticity of  $\pm \frac{1}{3}$ . The stripe pattern of OAM moments is the only possibility to satisfy this requirement. The stripe phase obtained here is quite general: for example, it will also appear in the triangular-lattice

$p + ip$  Josephson-junction array [13] if tunneling is dominated by the momentum-reversing process [20], rather than by the momentum-conserving process that gives a uniform state. This stripe ordering possibility in the triangular  $p + ip$  Josephson junction arrays has not been earlier appreciated.

In addition, the stripe order results in the staggered bond currents. We further optimize the  $U(1)$  phase variables, and find that their pattern is the same as that in the weak coupling limit. Taking into account the equal weight of  $p_{x,y}$  in each site, we find no phase mismatch along each horizontal bond, but a phase mismatch of  $\Delta\theta = \frac{\pi}{6}$  along each tilted bond. As a result, on each bond around the rhombic plaquette, the Josephson current is  $j = \frac{tn_0}{2} \sin \Delta\theta$  where  $n_0/n$  is the condensate fraction, and the current direction is specified by arrows in Fig. 1. The total phase winding around each rhombic plaquette is  $4\Delta\theta = \frac{2}{3}\pi$ , and thus agrees with the vorticity of  $\frac{1}{3}$ . We emphasize that the  $p$ -band square lattice case does not have this interesting physics [11].

Since the stripe order exists in both strong and weak coupling limits, it should also exist at intermediate coupling strength. We have confirmed this conjecture using the Gutzwiller mean field (GMF) theory in a  $30 \times 30$  lattice for three systems (marked as points 1, 2, and 3 in Fig. 2). We find that the stripe ordered ground state is stable against small perturbations in all three cases. We further apply the GMF theory to the  $2 \times 2$  unit cell (Fig. 1), and obtain the phase diagram of the stripe ordered SF and MI phases (Fig. 2A). To understand the GMF numerical results, we write the trial condensate with the  $p$ -orbital configuration on each site as  $e^{i\phi_{\vec{r}}} (\cos \alpha |p_x\rangle + i\sigma_{\vec{r}} \sin \alpha |p_y\rangle)$ . It turns out that the pattern for the  $U(1)$  phase does not depend on  $\alpha$ , and remains the same for all the coupling strength. The phase mismatch  $\Delta\theta$  on the tilted bonds reads  $\Delta\theta = 2\gamma - \pi/2$  with  $\tan \gamma = \sqrt{3} \tan \alpha$ , and the corresponding Josephson current is  $j = n_0 t \sin \Delta\theta$ . The value of  $\alpha$  is determined by the minimization of the energy per particle of the trial condensate as

$$\mathcal{E}(\alpha) = -t[1 + 2 \sin(2\alpha + \frac{\pi}{6})] - \frac{nU}{6} \sin^2 2\alpha + \frac{nU}{3}. \quad (5)$$

In the strong (weak) coupling limit, the energy minimum is located at  $\alpha = \frac{\pi}{4}$  ( $\frac{\pi}{6}$ ), and thus the flux in each rhombic plaquette  $\Phi = 4\Delta\theta/(2\pi) = 0$  ( $\frac{1}{3}$ ), which agrees with the previous analyses. For the intermediate interaction, we present both results of  $\Phi$  at  $n = 3$  based on the GMF theory and Eq.(5) in Fig. 2B. They agree with each other very well, and confirm the validity of the trial condensate. Moreover, in the momentum space, the trial condensate for a general  $\alpha$  can be expressed as  $\frac{1}{\sqrt{N_0!}} \left\{ \frac{1}{\sqrt{2}} (\psi'_{K_2} + i\psi'_{K_3}) \right\}^{N_0} |0\rangle$ , where  $\psi'_{K_{2,3}}(\vec{r}) = e^{i\vec{K}_{2,3} \cdot \vec{r}} |\phi_{2,3}(\alpha)\rangle$  with  $|\phi_{2,3}(\alpha)\rangle = -\cos \alpha |p_x\rangle \mp \sin \alpha |p_y\rangle$  respectively.

The OAM is of the Ising type, thus the stripe ordering is robust against small perturbations such as a small

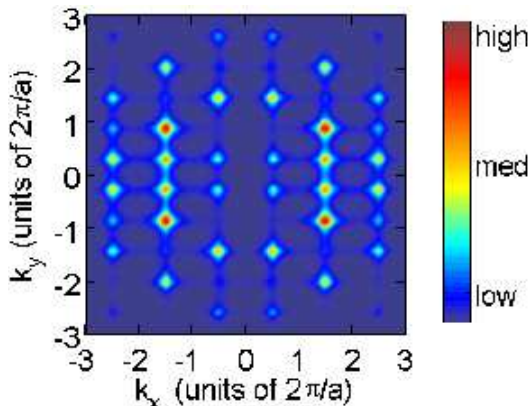


FIG. 3: Predicted TOF image for the stripe-ordered superfluid phase with the condensation wavevectors  $K_{2,3}$ . Note that the locations of the highest peaks depend on the size  $l_{x,y}$  of the  $p$ -orbital Wannier function. Parameters are:  $\alpha = \pi/6$ ;  $l_{x,y}/a = 0.1$ ; the  $\delta$ -function is replaced by a Lorentzian line for display.

value of the  $\pi$ -type bonding  $t_{\perp} \ll t_{\parallel}$ . Further, we also check that the phase pattern in Fig. 1 remains unchanged from minimizing the ground state energy. In particular, in the weak-coupling limit, the band minima and corresponding eigenvectors do not change at all in the presence of a small  $t_{\perp}$ , which renders the above conclusion obvious.

The formation of the on-site orbital moment does not depend on the inter-site phase coherence, and thus the Ising variables can be ordered even in the MI state. We performed a ring exchange analysis showing the existence of the stripe-ordering at  $n \geq 2$  provided the screening length of the interaction among vortices is larger compared to the size of the four-site plaquette. Due to loss of the inter-site phase coherence, bond currents disappear in the MI phase.

Our predicted stripe phase should manifest itself in the time of flight (TOF) signal as depicted in Fig. 3. In the SF state, we assume the stripe ordering wavevector  $K_1$ , and the corresponding condensation wavevectors at  $K_{2,3}$ . As a result, the TOF density peak position after a flight time of  $t$  is shifted from the reciprocal lattice vectors  $\vec{G}$  as follows

$$\langle n(\vec{r}) \rangle_t \propto \sum_{\vec{G}} \left\{ |\phi_2(\alpha, \vec{k})|^2 \delta^2(\vec{k} - \vec{K}_2 - \vec{G}) + |\phi_3(\alpha, \vec{k})|^2 \delta^2(\vec{k} - \vec{K}_3 - \vec{G}) \right\}, \quad (6)$$

where  $\vec{k} = m\vec{r}/(\hbar t)$ ;  $\phi_{2,3}(\alpha, \vec{k})$  is the Fourier transform of the Wannier  $p$ -orbital wavefunction  $|\phi_{2,3}(\alpha)\rangle$ , and  $\vec{G} = \frac{2\pi}{a}[m, (-m+2n)/\sqrt{3}]$  with  $m, n$  integers. Thus Bragg peaks should occur at  $\frac{2\pi}{a}[m \pm \frac{1}{2}, \frac{1}{\sqrt{3}}(-m+2n+\frac{1}{2})]$ . Due to the form factors of the  $p$ -wave Wannier orbit wavefunction  $|\phi_{2,3}(\alpha, \vec{k})|^2$ , the locations of the highest peaks is not located at the origin but around  $|k| \approx 1/l_{x,y}$ . Due

to the breaking of lattice rotation symmetry, the pattern of Bragg peaks can be rotated at angles of  $\pm \frac{2\pi}{3}$ . In the MI phase, Bragg peaks disappear due to the loss of phase coherence. Instead, the stripe order appears in the noise correlations  $\langle n(\vec{r})n(\vec{r}') \rangle$ , which exhibit not only the usual peaks at  $\vec{G}$ , but also peaks located at  $\vec{K}_1 + \vec{G}$ .

In summary, optical lattices provide a promising direction to study new phases of orbital physics. We focus on the  $p$ -band bosons in the frustrated triangular lattice which exhibits novel stripe orbital ordering of the on-site OAM due to the geometric frustration effect to the phase coherence. In the SF phase, the staggered plaquette bond currents are also induced, reminiscent of the  $d$ -density wave proposal for the pseudogap phase in high  $T_c$  cuprates [21] but with completely different microscopic origin. The stripe order persists in the MI phase even with the loss of superfluidity. The pattern of the stripe order can be observed in the TOF experiment. The orbital physics of cold atoms opens up intriguing problems yet to be explored, for example, the  $p$ -orbital ordering in other frustrated lattices such as the Kagome.

C. W. thanks L. M. Duan and T. L. Ho for helpful discussions. C.W. is supported by the the NSF Phy99-07949. W. V. L. is supported in part by ORAU Ralph E. Powe Award. J. E. M. is supported by NSF DMR-0238760. S. D. S. is supported by LPS-NSA.

- 
- [1] D. M. Stamper-Kurn *et al*, Phys. Rev. Lett. **80**, 2027 (1998); M. S. Chang *et al.*, Nature Physics, **1**, 111 (2005).
  - [2] T. L. Ho, *et al.*, Phys. Rev. Lett. **81**, 742(1998); T. Ohmi *et al.*, J. Phys. Soc. Jpn., **67**,1822 (1998); E. Demler *et al*, Phys. Rev. Lett. **88**, 163001(2002); F. Zhou, Phys. Rev. Lett. **87**, 80401(2001).
  - [3] C. Wu *et al.*, Phys. Rev. Lett. **91**, 186402 (2003).
  - [4] C. Wu *et al.*, cond-mat/0512602; T. L. Ho *et al.*, Phys. Rev. Lett. **82**, 247 (1999).
  - [5] C. Wu, Phys. Rev. Lett. **95**, 266404 (2005); P. Lecheminant *et al.*, Phys. Rev. Lett. **95**, 240402 (2005).
  - [6] Y. Tokura and N. Nagaosa, Science **288**, 462 (2000).
  - [7] A. Browaeys *et. al*, Phys. Rev. A **72** 53605 (2005).
  - [8] M. Kohl *et. al*, Phys. Rev. Lett. **94**, 80403 (2006).
  - [9] V. W. Scarola *et. al*, Phys. Rev. Lett. **65**, 33003 (2005).
  - [10] A. Isacsson *et. al*, Phys. Rev. A **72**, 053604 (2005).
  - [11] W. V. Liu and C. Wu, cond-mat/0601432.
  - [12] A. B. Kuklov, cond-mat/0601416.
  - [13] J. E. Moore *et al.*, Phys. Rev. B **69**, 104511 (2004).
  - [14] C. Xu *et al.*, Phys. Rev. Lett. **93**, 47003(2004).
  - [15] Z. Nussinov, *et. al*, Phys. Rev. B **71**, 195120 (2005).
  - [16] D. Jaksch and P. Zoller, Ann. Phys. **315**, 52 (2005).
  - [17] S. Mori *et al.*, Nature **392**, 473 (1998).
  - [18] J. Zaanen *et al.*, Phys. Rev. B **40**, 7391 (1989); S. A. Kivelson, *et al.*, Rev. Mod. Phys. **75**, 1201 (2003).
  - [19] M. P. Lilly *et al.*, Phys. Rev. Lett. **82**, 394 (1999) ;R. Du *et al.*, Solid State Commun. **109**, 389 (1999).
  - [20] C. Castelnovo *et al.*, Phys. Rev. B **69**, 104529 (2004).
  - [21] S. Chakravarty *et al.*, Phys. Rev. B **63**, 94503 (2001).